© 2021. Published by The Company of Biologists Ltd | Journal of Experimental Biology (2021) 224, jeb242903. doi:10.1242/jeb.242903

RESEARCH ARTICLE

Motor control in the epaxial musculature of bluegill sunfish in feeding and locomotion

Yordano E. Jimenez*,‡ and Elizabeth L. Brainerd

ABSTRACT

Fishes possess an impressive repertoire of feeding and locomotor behaviors that in many cases rely on the same power source: the axial musculature. As both functions employ different skeletal systems, head versus body, integrating these functions would likely require modular motor control. Although there have been many studies of motor control in feeding or locomotion in fishes, only one study to date has examined both functions in the same individuals. To characterize bilateral motor control of the epaxial musculature in feeding and locomotion, we measured muscle activity and shortening in bluegill sunfish (*Lepomis macrochirus*) using electromyography and sonomicrometry. We found that sunfish recruit epaxial regions in a dorsal-to-ventral manner to increase feeding performance, such that high-performance feeding activates all the epaxial musculature. In comparison, sunfish seemed to activate all three epaxial regions irrespective of locomotor performance. Muscle activity was present on both sides of the body in nearly all feeding and locomotor behaviors. Feeding behaviors used similar activation intensities on the two sides of the body, whereas locomotor behaviors consistently used higher intensities on the side undergoing muscle shortening. In all epaxial regions, fast-starts used the highest activation intensities, although high-performance suction feeding occasionally showed near-maximal intensity. Finally, active muscle volume was positively correlated with the peak rate of body flexion in feeding and locomotion, indicating a continuous relationship between recruitment and performance. A comparison of these results with recent work on largemouth bass (*Micropterus salmoides*) suggests that centrarchid fishes use similar motor control strategies for feeding, but interspecific differences in peak suction-feeding performance are determined by active muscle volume.

KEY WORDS: Muscle activity, Swimming, Suction feeding, C-starts, Fast-starts, Performance

INTRODUCTION

Motor control makes muscle functionally versatile, enabling animals to match their movements to a wide range of physical and environmental conditions. Variable muscle recruitment can adjust the speed, force and direction of movement, and altogether change what type of behavior is produced (Biewener and Corning, 2001; Ellerby et al., 2001; Jimenez and Brainerd, 2020). For example, monitor lizards vary the activity of red and white muscle fibers to maintain similar locomotor speeds despite temperature changes that are expected to have detrimental effects on locomotor performance (Jayne et al., 1990). Golden-colored manakins alter the activation patterns of flight muscles during courtship displays to produce audible snaps with their wings – a behavior markedly different from powered flight (Fuxjager et al., 2017). Thus, comparing the activation patterns of muscle under various conditions and during different behaviors can elucidate the functional versatility, specialization, limitations and evolution of muscle.

In fishes, the axial musculature is equipped with a neural circuitry that enables most species to switch seamlessly between distinct mechanical tasks: axial locomotion and suction feeding (Jimenez and Brainerd, 2020). Axial locomotion involves lateral body bending produced by alternating contractions of the left and right sides of the axial musculature. In contrast, suction feeding involves rapid cranial expansion that is typically, through numerous musculoskeletal linkages in the skull, driven by neurocranial elevation from the pull of the epaxials, and/or pectoral girdle retraction from the pull of the hypaxials (Camp and Brainerd, 2014; Camp et al., 2018, 2020; Van Wassenbergh et al., 2005). This configuration enables the axial muscles to generate over 90% of suction power routinely (Camp et al., 2015, 2018; Jimenez and Brainerd, 2020). These starkly different behaviors involving different musculoskeletal regions, the head and the body, are united by a common power source, and the emerging challenge is to determine the mechanical and evolutionary implications of such a dual-function muscle. A critical first step in this effort is to quantify the motor control patterns that have integrated these two musculoskeletal systems. To do so, it is necessary to first review motor control of axial locomotion and feeding in fishes.

Fishes use several recruitment strategies to adjust the performance of axial locomotion. The first strategy recruits muscle in order of fiber type, where the progression of muscle activation starts with slow-twitch muscle (small red fibers) and ends with fast-twitch muscle (large white fibers), a phenomenon known as the size principle (Boddeke et al., 1959; Bone et al., 1978; Henneman, 1957; Henneman et al., 1965). Consequently, fish generally activate only red muscle fibers at low swimming speeds but at some threshold begin activating white muscle fibers, increasing the number of active white fibers to increase tailbeat frequency (Bone et al., 1978; Jayne and Lauder, 1994; Jimenez and Brainerd, 2020; Johnston et al., 1977). This pattern is also observed in fish species with pink muscle fibers, with an intermediate stage of pink fiber activation between red and white fiber activation (Coughlin and Rome, 1996; Johnston et al., 1977). Once white muscle fibers are recruited, subsequent increases in performance are produced not by activating different fiber types but by activating a greater number of white fibers (Bello-Rojas et al., 2019; Jimenez and Brainerd, 2020; McLean et al., 2007), which comprise 75–100% of the muscle's cross-sectional area (Boddeke et al., 1959; Greer-Walker and Pull, 1975). For example, largemouth bass

Department of Ecology and Evolutionary Biology, Brown University, 80 Waterman Street, Providence, RI 02912, USA.
*Present address: Department of Biology, Tufts University, Medford, MA 02155, USA.

‡Author for correspondence (jimenez.yordano@gmail.com)

Y.E.J., 0000-0001-5200-399X; E.L.B., 0000-0003-0375-8231

Received 25 May 2021; Accepted 20 September 2021

(*Micropterus salmoides*) vary swimming performance by activating muscle in a ventral-to-dorsal progression, where low-frequency sprinting recruits only the ventral epaxial regions, and high-frequency sprinting activates both the ventral and dorsal epaxial regions (Jimenez and Brainerd, 2020). At the peak of locomotor performance, evasive and predatory fast-starts, fishes can recruit the totality of fibers in all regions of the axial musculature (Ellerby and Altringham, 2001; Jimenez and Brainerd, 2020; Lauder, 1980; Liu and Hale, 2014; Tytell and Lauder, 2002; Westneat et al., 1998). Underlying these complex activation patterns is a motor pool composed of spatially diverse motor units that, depending on the behavior, can independently activate different muscle regions and different numbers of muscle fibers within those regions (Bello-Rojas et al., 2019; McLean et al., 2007).

Suction-feeding fishes use the same axial motor pool for both locomotion and feeding and can modulate performance and function with variable white muscle activity. Largemouth bass increase suction-feeding performance via incremental recruitment of different epaxial regions (Jimenez and Brainerd, 2020) and increased activation intensity (Carroll and Wainwright, 2006; Jimenez and Brainerd, 2020). An important difference is that the progression of muscle recruitment is inverted in suction feeding, such that muscle activity starts dorsally and progresses ventrally. For example, low-motivation strikes on pellet food partially recruit the dorsal region, but high-motivation strikes on live prey are more likely to partially recruit all epaxial regions. Unlike locomotion, suction feeding in largemouth bass exhibits a rostrocaudal recruitment pattern where low-performance strikes activate rostral muscle, but high-performance strikes activate rostral, midbody and caudal muscle (Jimenez and Brainerd, 2020; Thys, 1997). Until now, axial motor control as a dual-function phenomenon has only been studied directly in one species, largemouth bass (Jimenez and Brainerd, 2020). Neuroanatomical similarities across fish taxa would suggest fishes share the capacity to modulate behavior and performance with similar motor control strategies, but good reasons exist to expect variability.

Fishes exhibit a wide range of variability in suction-feeding performance (Carroll et al., 2004; Longo et al., 2016; Oufiero et al., 2012), and the mechanical contributions of the axial musculature to suction feeding can vary by species (Camp et al., 2020). Thus, some species generate high suction expansion power relative to body mass, whereas others do not (Camp et al., 2020). For example, largemouth bass use very low activation intensities (Jimenez and Brainerd, 2020) and generate only a fraction of the muscle's theoretical maximum power in suction feeding (Camp et al., 2015; Carroll et al., 2009). In contrast, bluegill sunfish routinely generate very high muscle power outputs, up to 438 W kg^{-1} (Camp et al., 2018). The varying mechanical contribution of the axial musculature to suction feeding raises the question: what is responsible for interspecific and intraspecific differences in suction-feeding power?

The objectives of this study were threefold. (1) Determine whether the dual-function recruitment patterns found in bass also exist in a closely related species with a different body shape, ecological niche and feeding strategy (Higham, 2007; Norton and Brainerd, 1993). Is there evidence that the observed recruitment patterns in suction feeding are preserved? (2) Assess muscle recruitment in a species that produces high muscle power for suction feeding compared with largemouth bass. Can a species that generates high suction expansion power relative to its body mass recruit a greater cross-sectional area of the musculature to generate higher power outputs? (3) Quantify and compare the bilateral muscle activity between locomotor and feeding behaviors in the same set of experimental animals. Is muscle activity bilaterally symmetrical for suction feeding and bilaterally asymmetrical for swimming?

MATERIALS AND METHODS

Animals

Bluegill sunfish (*Lepomis macrochirus* Rafinesque 1819) were caught at Lake Waban in Wellesley, MA, USA. Fish (standard length, SL: 173, 171, 164 and 161 mm for Lm01, Lm02, Lm03 and Lm04, respectively) were housed at Brown University in tanks at room temperature (19–21°C). We acclimated the fish for a minimum of 6 weeks, during which time they were trained to feed on carnivore pellets and live prey, such as goldfish (*Carassius auratus*) and rosies (*Pimephales promelas*). Two weeks before surgery and experimentation, we fed the fish less frequently, and eventually not at all, to increase their appetite. All procedures were approved by and followed the policies of the Institutional Animal Care and Use Committee (IACUC) of Brown University.

Experimental design

To detect disparities in muscle activity related to function and performance, we recorded EMGs and muscle strain during feeding and locomotion at a range of performance levels. To elicit a range of feeding performance levels, we fed the sunfish carnivore pellets and live prey (goldfish and rosies) as prior studies have documented that fish suction feed on elusive prey at higher performance levels (Jimenez and Brainerd, 2020; Nemeth, 1997; Norton and Brainerd, 1993). Sunfish were fed pellets and live prey in haphazard order to ensure that differential performance was associated with food type and not with satiation during data collection. We analyzed data from successful and unsuccessful suction strikes. We used video footage to categorize behaviors and exclude trials with aberrant movements that could affect the EMG signal (e.g. fish bumping into the tank). To ensure that muscle activity during suction feeding was not confounded with locomotor activity, we used a combination of video and sonomicrometry data to exclude trials with substantial lateral body flexion during the strike. To record a range of locomotor performance levels, we used hand movements of varying intensity in the water to elicit three types of burst swimming: turns, sprints and fast-starts. All three burst swimming behaviors use white muscle fibers, but they differ in their mechanics and intensity. We categorized turns and sprints as lower-performance behaviors and fast-starts as a high-performance behavior. We recorded a range of tail beat frequencies (3–22 Hz, based on the duration of muscle shortening) comparable to the range of frequencies recorded in largemouth bass (Jimenez and Brainerd, 2020) and other fish species similar in length to our sunfish (Bainbridge, 1958; Wardle, 1975), suggesting that we indeed elicited strong sprinting performance. All feeding and swimming trials were done in a 60 gallon tank with dimensions 48×13×22 inches (~122×33×56 cm, length×width×height).

Electrode construction

Bipolar electrodes were constructed from 0.1 mm diameter, Teflon-insulated stainless-steel wire (A-M Systems, Sequim, WA, USA). We twisted together two wires and added a tighter twist to the last ~3 cm on the recording end, where we offset the tips by 3 mm. After offsetting the wires, we removed approximately 1 mm of insulation from the tip of the recording end for each wire. Connector pins were soldered onto the connector ends of the wire. The recording end of the bipolar electrode was placed inside the beveled opening of a 23-gauge hypodermic needle and bent back to form a hook, allowing the leads with connector pins to hang on the outside of the needle.

Journal of Experimental Biology (2021) 224, jeb242903. doi:10.1242/jeb.242903

Surgical procedures

Prior to each surgery, we anesthetized and CT (computed tomography) scanned each individual *in vivo* and took measurements of the intended implantation sites. Fish were anesthetized via immersion in 0.12 g l^{-1} buffered MS-222 (tricaine methanesulfonate). We then placed the fish in a surgical tray with a flow of anesthetic solution and intubated the mouth to flow oxygenated water over the gills. For each sonomicrometry transducer (4 total per individual), we removed scales from the implantation site, made a small dermal incision (1 mm), and used a 16-gauge needle with a blunted tip to make a path for the transducer–holder unit (see below). We then sutured the external arms of the holder onto the skin. Electrodes (6–8 per individual but only 6 were analyzed in this study) were then percutaneously implanted through the soft tissue between the scales to a depth halfway between the skin and the vertical septum. The electrode and sonomicrometer leads exiting from the muscle were glued together (E600 flexible craft adhesive) to form a common cable, which we then sutured onto the region above the head to relieve any tension from the lead wires and to prevent them from dislodging from the animal.

Implantation sites

Electrodes were implanted in a total of six positions in each sunfish at ∼35% SL (Fig. 1A). Three electrodes were implanted on each side of the body, each dorsoventral location corresponding to different myomeric regions of the epaxial musculature: the dorsal-pointing arm (DPA), the posterior-pointing cone (PPC) and the anterior-pointing cone (APC), anatomical regions which also approximate the territories of distinct motoneurons (Fig. 1B; Bello-Rojas et al., 2019). Sonomicrometry transducers were positioned to measure longitudinal strain of the epaxial muscle mass at different distances from the neutral axes of bending, not to measure strain within a single myomere or measure muscle fiber strain along the white muscle fibers that typically lie at various angles relative to the long axis of the body (Alexander, 1969; Gemballa and Vogel, 2002). Each sonomicrometry transducer was mounted on a custom-made stainless steel holder with three arms (Carr et al., 2011; Olson and Marsh, 1998) and the positioning of the holder on the transducer lead was used to implant the transducer at the desired muscle depth. We implanted two pairs of transducers (1 mm diameter) in the epaxial musculature on the left side of the body. Each pair was approximately 15 mm apart, with each unit on either side of the electrodes. Each pair was also oriented parallel to the long-axis of the animal, defined as a line going from the snout tip to the notch in the caudal fin. One pair was implanted dorsomedially at approximately 14 mm dorsal to the vertebral column and 3 mm lateral to the vertical septum. The other pair was implanted ventrolaterally at approximately 8 mm dorsal to the vertebral column and 5 mm lateral to the vertical septum (Fig. 1B). After each experiment, sunfish were CT scanned with a Fidex scanner (Animage, Pleasanton, CA, USA) at a 0.15 mm voxel resolution to confirm electrode and transducer positions.

Data collection and filtering

Trials were filmed from a lateral view and a dorsal or anterior view with a GoPro camera at a minimum of 60 frames s^{-1}. We synchronized EMG recordings with sonomicrometry recordings by sending a 1 Hz signal from the LabChart PowerLab (Model PL3516) to the sonomicrometry acquisition software. To synchronize data and video, this 1 Hz square wave signal was also sent to a flashing LED light in the field of view of the cameras. Video, EMG and sonomicrometry data for this publication have been deposited in the ZMAPortal (zmaportal.org) in the study 'Sunfish EMG and Sonomicrometry in Feeding and Locomotion' with permanent ID ZMA27. Video data are stored in accordance with best practices for video data management in organismal biology (Brainerd et al., 2017).

Electromyograms were amplified by 1,000 or 10,000, depending on signal strength, with low- and high-pass hardware filters set to 10 kHz and 100 Hz, respectively (A-M Systems, differential AC amplifier, model 1700). A 60 Hz hardware notch filter was also used to reduce noise from ambient AC circuits. Analog to digital conversion was done using PowerLab data acquisition hardware at a sampling frequency of 4 kHz, and EMGs were recorded in LabChart (AD Instruments, Sydney, NSW, Australia). EMG signals were rectified and software-filtered using the biosignalEMG package for R-studio (https://CRAN.R-project.org/package=biosignalEMG). Rectified data were processed with a Butterworth filter with low- and high-pass settings of 1 kHz and 100 Hz, respectively. Finally, we calculated the moving average (window of 5 frames or 1.25 ms) to create an envelope of the rectified-and-filtered signal for parts of the analysis.

Muscle length (L) data were recorded at a sampling rate of 1041 Hz in SonoLab software (version 3.4.81) using a Sonometrics system (Model TR-USB Series 8). We measured water temperature to get the muscle temperature in our ectothermic fish, and input the appropriate speed of sound at the beginning of each experiment to account for any temperature changes (Marsh, 2016). Post-processing of level shifts in the sonomicrometer signals was

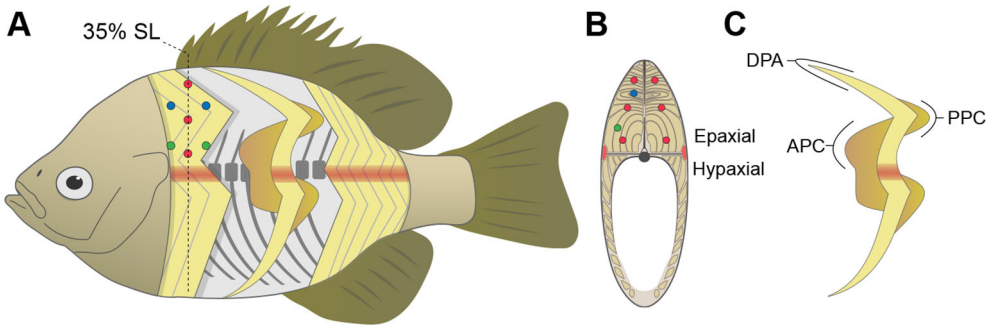

Fig. 1. Diagram of electrode and sonomicrometry transducer positions within the axial musculature. (A) Lateral and (B) transverse views of a bluegill sunfish showing the approximate positions of electrodes and sonomicrometry transducers implanted within the axial musculature, composed of serially repeating myomeres. Red circles show approximate electrode positions in the three epaxial regions at 35% standard length (SL) considered in this study. Blue and green circles show the positions of the two sonomicrometry transducer pairs used to measure muscle shortening. (C) Lateral view of an isolated myomere indicating the three epaxial regions examined in this study. APC, anterior-pointing cone; DPA, dorsal-pointing arm; PPC, posterior-pointing cone.

done in Igor Pro (Wavemetrics, Lake Oswego, OR, USA) and muscle length data were smoothed using the smooth.spline function in the stats package before and after calculating strain in R (http://www.R-project.org/). Initial muscle length (L_i) was defined as the muscle length (L) prior to the onset of the behavior and muscle shortening. Strain (E) was calculated as $(L-L_i)/L_i$. Muscle shortening velocity (L s^{-1}) was calculated as the time-derivative of strain.

Data analysis

We defined the on–off state of muscle based on a subjectively determined voltage threshold set for each channel, where muscle with a filtered peak voltage exceeding the threshold is considered active (i.e. above-threshold muscle activity). We used a manually selected time frame that approximates the duration of the ipsilateral activity to calculate peak voltage in the ipsilateral and contralateral sides. Thus, our detection of concurrent ipsilateral and contralateral muscle activity indicates some temporal overlap but does not imply the same onset and offset times, which we did not analyze in this study. We calculated normalized activation intensity in each electrode by dividing all voltage envelopes by the maximum voltage envelope recorded. We calculated active muscle volume by multiplying the normalized activation intensity of each muscle region (DPA, PPC and APC) by its percentage of epaxial cross-sectional area and adding all the values. Unless otherwise noted, we analyzed the activation intensities for feeding behaviors on the side with the highest value (left or right side of a given muscle region at any point during the strike). For locomotor behaviors, we calculated the normalized activation intensity and active muscle volume on the ipsilateral side at any point during muscle shortening.

Bilateral symmetry of normalized activation intensity was calculated for each trial by comparing values of each left–right electrode pair. As feeding and locomotion flex the body in different directions (Jimenez et al., 2021), we used different criteria to assess symmetry. For feeding, we used the peak normalized activation intensity at any point during the activity burst and a trial was counted as symmetrical if the pairwise difference of a left–right electrode pair did not exceed a tolerance level. Tolerance levels were set using the standard deviation for data aggregated by feeding behavior, individual and muscle region. For example, the standard deviation of normalized activation intensity for Lm01 within the DPA for live prey strikes was 22%, so a strike would be counted as symmetrical if the left and right electrodes of the DPA region of individual Lm01 had values within 22% (absolute percentage) of each other. For the same region and individual, the left–right intensities would have to be within 1.3% of each other for a chewing behavior because the standard deviation for that behavior was so much lower. We set the tolerance to 1% in cases where an electrode pair had standard deviations less than 1%, as we consider differences less than 1% to be negligible. For swimming, a trial was counted as asymmetrical only if ipsilateral activity, the side with active muscle shortening, was greater than contralateral activity at the time of peak ipsilateral activity. The tolerance level for asymmetry was set to 200% (relative percentage), such that the normalized activation intensity of the ipsilateral side had to be at least twice that of the contralateral side. For our analysis, trials with higher intensities on the contralateral side were classified as symmetrical, as they do not meet the *a priori* expectation that higher levels of muscle recruitment occur on the side toward which the fish bends.

In order to pool strain rate data from all individuals, we corrected our muscle strain measurements to account for differences caused by variable sonomicrometry transducer locations. Longitudinal muscle strain has been shown to vary with distance from the neutral axis of bending (i.e. the vertebral column) as a result of the beam-like deformation of fish muscle, where locomotion produces a mediolateral gradient and feeding produces a dorsoventral gradient (Jimenez et al., 2021). Assuming that the strain gradient is linear and that strain is zero at the vertebral column, we applied the following correction factor: $E_{estimated}=E_{measured}\times(Z_{measured}/Z_{estimated})$, where $E_{measured}$ is the strain measured by a transducer pair, $Z_{measured}$ is the linear distance of the transducer pair from the neutral axis, and $Z_{estimated}$ is the distance from the neutral axis for which an estimate of longitudinal muscle strain is desired. We applied this correction factor to all individuals to estimate strain at the furthest point from the neutral axis of each function. After correcting strain data for variable positions, we pooled data from all individuals and calculated rate of body flexion for feeding and locomotion by dividing peak strain rates by the greatest rate measured in each function. Relative rate of body flexion provided a continuous measure of performance that avoided the confounding factors associated with using strain measurements to analyze the performance in these functions: (1) different strain gradients and muscle distributions with respect to the neutral axes of feeding and locomotion (Jimenez et al., 2021) and (2) unknown gearing of the oblique axial muscle fibers (Gemballa and Vogel, 2002).

Statistical analysis

Statistical analyses, including linear regressions, eta-squared test of variance, ANOVA and Tukey *post hoc* tests were performed in R using its native functions (http://www.R-project.org/). ANOVA with significant results were followed up with Tukey's HSD *post hoc* tests. For all tests, a P-value <0.05 was considered statistically significant. Owing to uneven sample sizes across individuals and behaviors, the percentage of trials with bilateral symmetry were aggregated by individual, behavior, function (feeding or locomotion) and muscle region for statistical analysis.

RESULTS

Muscle strain and activation

The epaxial musculature actively shortened in both feeding and locomotor behaviors (Fig. 2). In both behaviors, muscle activation began prior to the onset of muscle shortening. An example suction strike on a live prey (Fig. 2A) shows the onset of simultaneous bilateral muscle activation in all epaxial regions promptly followed by rapid muscle shortening. We observed pre-lengthening in some strikes, typically those on live prey. The example fast-start (Fig. 2B) shows bilateral asymmetry of muscle activity, where stage-1 muscle activity is prominent ipsilaterally (the side of the body undergoing muscle shortening), followed by prominent contralateral muscle activity that begins just prior to stage 2. Muscle strain data in this study were used to confirm that muscle produced positive mechanical work and, in conjunction with video recordings, to distinguish behaviors and their directionality. Strain data helped distinguish between stage 1 and stage 2 of the fast-start and determine which side of the axial musculature was actively shortening during sprints and turns.

Regional muscle activation

During feeding, the presence or absence of muscle activity varied with epaxial region and feeding behavior (Fig. 3A). On average, the percentage of trials with above-threshold muscle activity was highest in the dorsal-most region (dorsal-pointing arm, DPA), intermediate in the middle region (posterior-pointing cone, PPC) and lowest in the ventral-most region (anterior-pointing cone, APC).

Journal of Experimental Biology (2021) 224, jeb242903. doi:10.1242/jeb.242903

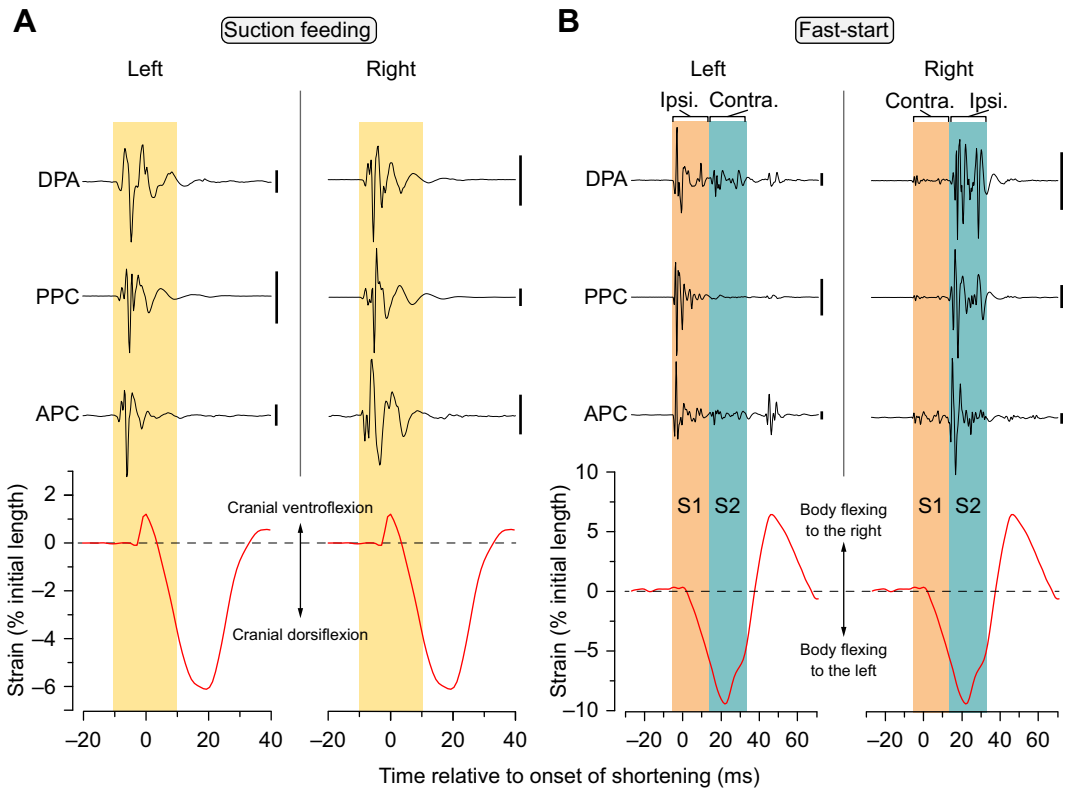

Fig. 2. Muscle activity and shortening for high-performance suction feeding and swimming. EMG traces from different sides of the body (left, right) for the different epaxial regions (dorsal to ventral: DPA, PPC, APC). (A) Muscle activity in the left and right sides of the body during a suction strike on live prey, with muscle strain measured with sonomicrometry transducers positioned in the dorsomedial muscle. (B) Muscle activity in the ipsilateral and contralateral sides of the body during a fast-start, with muscle strain measured with sonomicrometry transducers positioned in the ventrolateral muscle. Scale bars to the right of each trace are 1 mV. S1, stage 1; S2, stage 2.

Although differences were not always statistically significant, mean percentage decreased from dorsal to ventral for all feeding behaviors on both sides of the body. Furthermore, the averages were consistently highest in live prey strikes, intermediate in pellet strikes and lowest in chews. All individuals activated the DPA more frequently for suction feeding (live prey and pellet strikes) than for chewing, except for the left DPA in Lm03. Ventral muscle regions (PPC and APC) were also activated more frequently for live prey

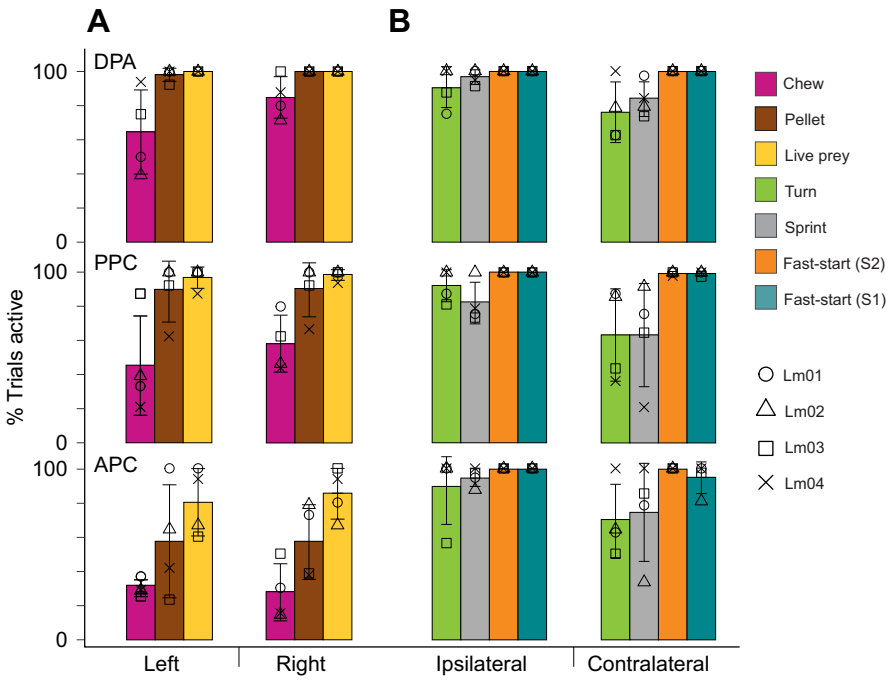

Fig. 3. Percentage of trials with above-threshold muscle activity in different epaxial regions for different behaviors. (A) Feeding behaviors. (B) Locomotor behaviors. Each plot shows data for a different epaxial region (dorsal to ventral: DPA, PPC, APC) and side of the body. Each bar is the mean±s.d. of the percentage values from all four individuals (symbols). See Fig. 5 for number of trials for each individual and behavior category.

Journal of Experimental Biology (2021) 224, jeb242903. doi:10.1242/jeb.242903

strikes than for pellet strikes and chews. Across locomotor behaviors, the percentage of trials with above-threshold ipsilateral muscle activity varied with behavior but not by region (Fig. 3B). Stage-1 and stage-2 fast-starts activated ipsilateral muscle in 100% of trials and contralateral muscle in over 95% of trials. In contrast, contralateral muscle activity was present in over 21% of sprints and in over 36% of turning maneuvers for each of the three regions.

Bilateral symmetry of activation intensity

Muscle activity was frequently observed in both sides of the body during both feeding and locomotion (Fig. 3), so we compared activation intensity in the different sides of the body. Intensity was bilaterally symmetrical in feeding, i.e. similar intensities within the left and right sides of a muscle region, but asymmetrical in axial locomotion, i.e. higher intensities in the intensities muscle region relative to the contralateral side (Fig. 4). Feeding behaviors used bilaterally symmetrical activation intensities at a much greater frequency than locomotion (Fig. 4; factorial ANOVA with function, individual and muscle region as factors, $P<0.001$). Bilateral symmetry was significantly affected by function – feeding or locomotion – in all three muscle regions (factorial ANOVA followed by Tukey *post hoc* tests, $P<0.001$). Other factors and interactions between factors also had a statistically significant effect on bilateral symmetry (function×region, function×individual, function×region×individual), but when combined they explained only 14% of variance, whereas function alone explained 72% of variance (partial eta-squared test). Data pooled by function alone showed that 86% of feeding observations were symmetrical (601 of 702; 234 feeding trials×3 muscle regions=702 total), whereas only 16% of locomotor observations were categorized as symmetrical using our conservative estimate of locomotor symmetry (218 of 1329; 443 locomotion trials×3 muscle regions=1329 total).

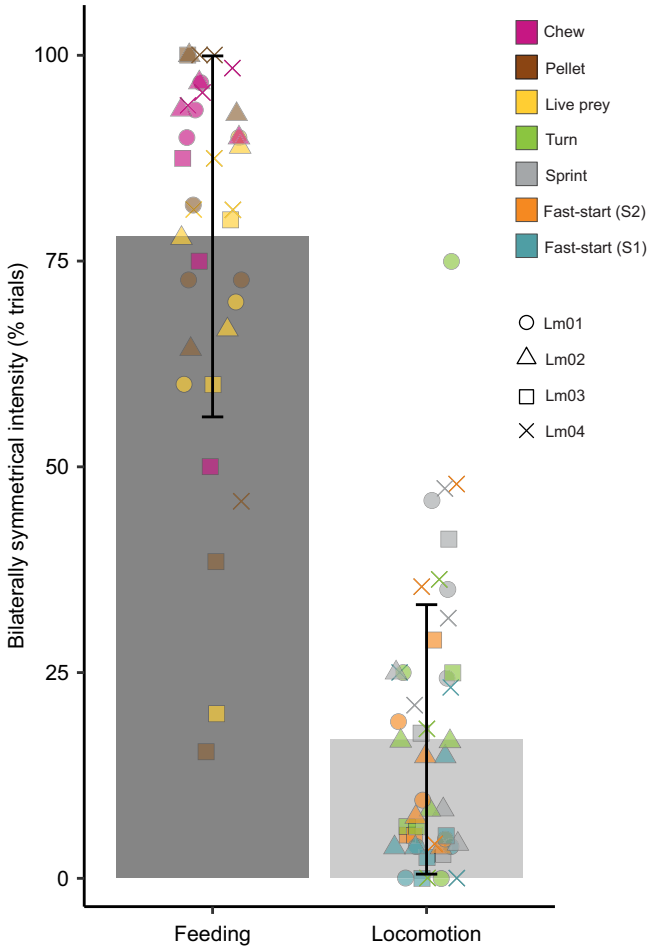

Fig. 4. Bilateral symmetry of activation intensity for feeding and locomotion. Bars show the mean±s.d. of aggregate data for each function, as distinguished by the direction of axial flexion and the expected symmetry of muscle activity. Each point is the left–right electrode pair of an epaxial muscle region (not indicated) within a particular individual (symbol) for a given behavior (color). Symmetry in feeding and locomotion were assessed by different metrics suitable for each function (see Materials and Methods for description). See Fig. 5 for number of trials for each individual and behavior category.

Normalized activation intensity

Muscle activation intensity was significantly affected by behavior, accounting for 57% of the variance in activation intensity (Fig. 5; factorial ANOVA, $P<0.01$; eta-squared test of variance). Other significant effects included individual, and behavior×region, behavior×individual and region×individual interactions ($P<0.01$), but combined accounted for less than 3% of the variance (eta-squared test of variance). Region alone and region×individual×behavior interactions had no statistically significant effect on activation intensity. Mean±s.d. normalized activation intensity for pooled data grouped only by behavior were from highest to lowest: stage-1 fast-starts (54±27%), stage-2 fast-starts (33±25%), prey strikes (17±20%), turns (4±5%), sprints (3±5%), pellet strikes (2±2%) and chews (1±2%).

We performed a Tukey *post hoc* test to determine which interactions between individual, region and behavior were statistically significant. Prey strikes had higher mean activation intensities than pellet strikes and chews in all three epaxial regions for all individuals, including Lm02, where the average differences were smaller. However, these differences were only statistically significant in two cases: the prey strike–chew comparison in the DPA of Lm01 and Lm04. Pellet strikes and chews used statistically similar intensities across all epaxial regions and individuals. Prey strikes and stage-1 fast-starts used statistically similar activation intensities in 5 of 12 cases: the DPA and PPC of Lm01 and Lm03, and the APC of Lm03. In the other 7 cases, stage-1 fast-starts used statistically higher activation intensities than prey strikes. Activation intensities were also statistically similar in prey strikes and stage-2 fast-starts in 10 of 12 cases, except for the PPC and APC of Lm02, where activation intensities were statistically greater for stage-2 fast-starts. Prey strikes were in all cases statistically similar to sprints and turns. Within each muscle region of each individual, stage-1 fast-starts used statistically higher activation intensities than both sprints and turns, and stage-2 fast-starts used statistically higher activation intensities than sprints. Stage-2 fast-starts used statistically higher activation intensities than turns in 10 of 12 cases, those statistically non-significant being the DPA and APC of Lm04. We found no statistical differences between sprint and turn activation intensities for any region of any individual.

Active muscle volume

Active muscle volume was significantly correlated with peak rate of body flexion in feeding and locomotion (Fig. 6). Both biological functions had moderate to strong positive logarithmic relationships between active muscle volume in both sides of the body and rate of flexion, where the effects of active muscle volume on rate of flexion decreased as active muscle volume increased. For feeding, the relationship between active muscle volume and body flexion rate was very similar in the left and right sides of the body even though

Journal of Experimental Biology (2021) 224, jeb242903. doi:10.1242/jeb.242903

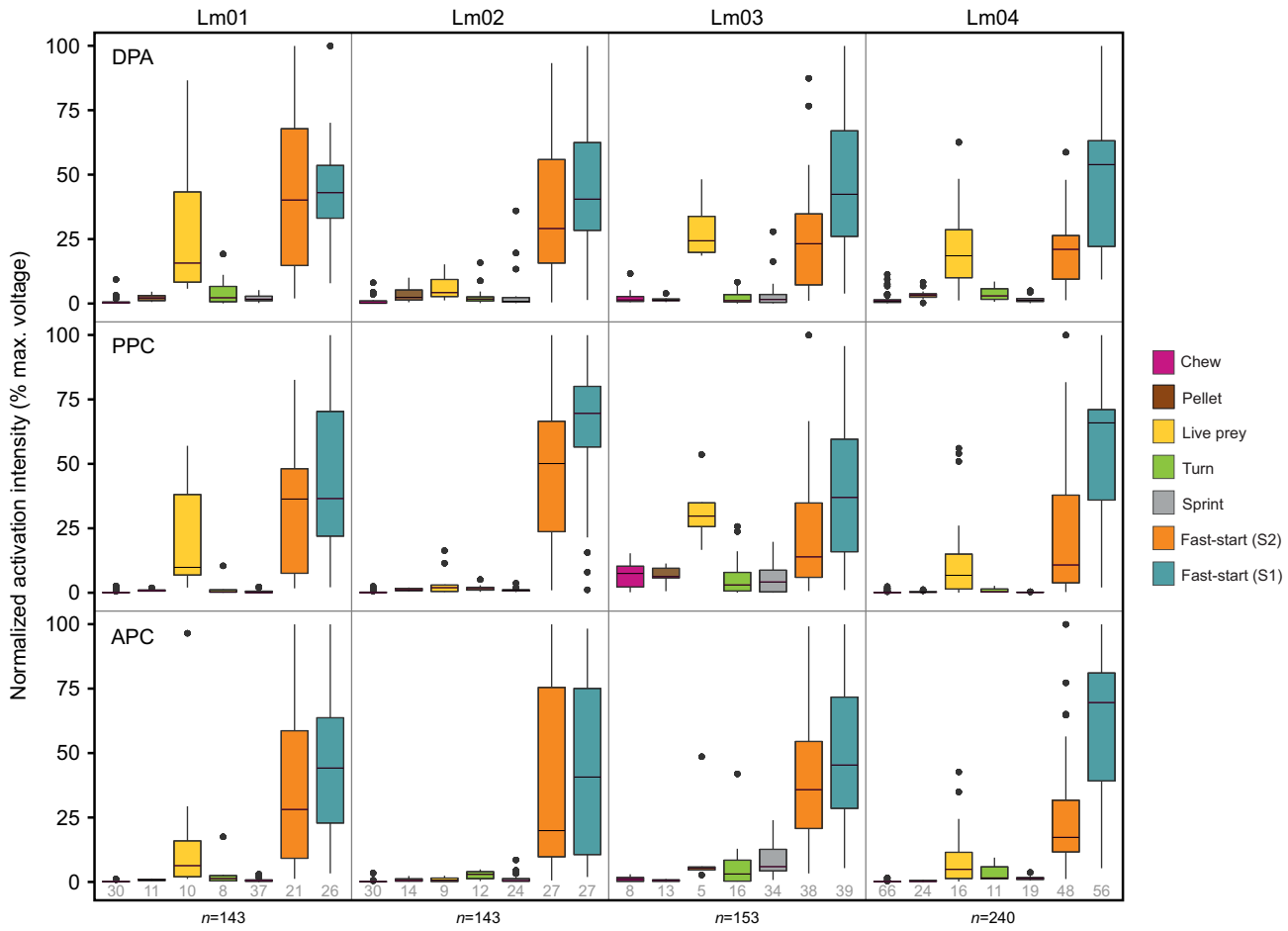

Fig. 5. Normalized muscle activation intensity for each individual, region and behavior. Activation intensity for each electrode was calculated by dividing all voltages by the peak fast-start voltage, the highest voltage. Data are shown for each individual (Lm01–04) for the different dorsoventral muscle regions. For swimming, activation intensity is always for the side of muscle shortening (e.g. left electrodes for a left body bend). For feeding, the side with the highest activation intensity was used. Successful and unsuccessful suction-feeding strikes are included in this analysis. For each colored box, the horizontal line (median value) separates the second (top) and third (bottom) quartiles, while the top and bottom error bars are the first and fourth quartiles, respectively, and individual points are outliers (defined as points above or below the interquartile range by a factor of 1.5). The number of trials for each individual and behavior category is listed at the bottom and was the same number for all analyses in this study.

strain, from which we calculated rate of flexion, was measured only in the left side. A similar relationship was found in locomotion, though the regressions for the left and right sides had different shapes (Fig. 6C,D). The different shapes of these regressions may be due to behavioral changes in response to the heavier instrumentation on the left side of the body or an error associated with estimating rate of body flexion for rightward movements with sonomicrometry transducers located in the left side of the body.

Active muscle volume was also correlated with categorical variables in bluegill sunfish and largemouth bass (re-analyzed data from Jimenez and Brainerd, 2020). Behavior had a statistically significant and primary effect on the active muscle volume in both species, accounting for 73% of variance in bass and 59% of variance in sunfish (factorial ANOVA, $P<0.01$; eta-squared test). Within each species, all other significant and non-significant effects combined accounted for less than 4% of variation. Thus, we pooled all data to statistically test species differences in active muscle volume (Fig. 7). Behavior, species and behavior×species interactions all had statistically significant effects (factorial ANOVA, $P<0.01$) but behavior accounted for 60% of the variance (60%) as compared with 2% explained by the other two variables (eta-squared test). Sunfish and bass used similar activation intensities for each behavior except turns (Tukey *post hoc* test, $P<0.01$). In both species, stage-1 fast-starts activated significantly more muscle volume than all other behaviors, including stage-2 fast-starts. Stage-2 fast-starts activated significantly more muscle volume than all other behaviors, except stage-1 fast-starts.

DISCUSSION

Comparison of bluegill sunfish and largemouth bass

Muscle recruitment patterns of bluegill sunfish in feeding and locomotion show important similarities and differences to those of largemouth bass (Jimenez and Brainerd, 2020). As far as we know, these are the only two species in which muscle recruitment patterns have been recorded in the same individuals with the same electrodes in both behaviors, thereby allowing comparison between biological functions. Similarities between these species include: (1) dorsal-to-ventral activation of the epaxial musculature associated with increased feeding performance, (2) activation of all epaxial regions in fast-starts, and (3) substantially higher activation intensities for fast-starts than for all other behaviors. Differences between these species include: (1) sunfish did not show a strong ventral-to-dorsal activation pattern of muscle activity associated with swimming performance, whereas bass were less

Journal of Experimental Biology (2021) 224, jeb242903. doi:10.1242/jeb.242903

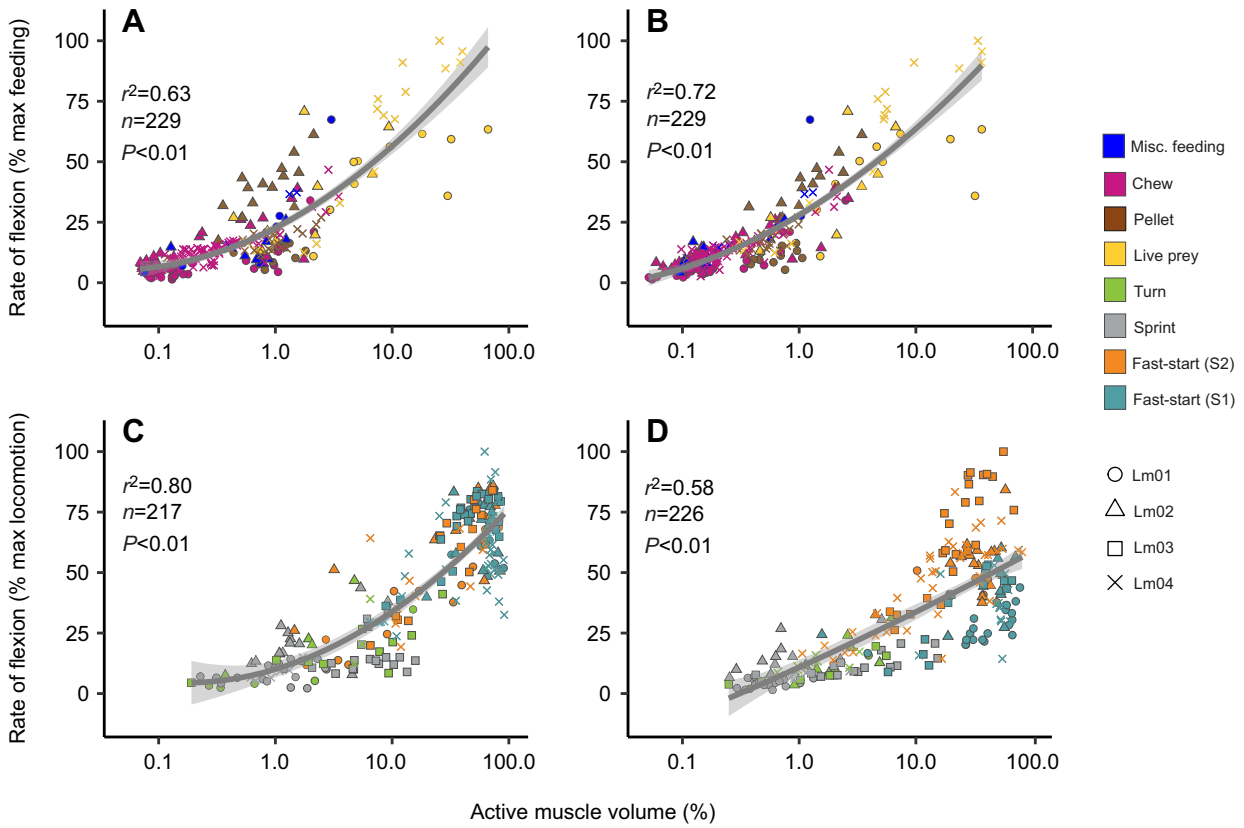

Fig. 6. Correlation between active muscle volume and peak rate of body flexion. (A,B) Feeding behaviors. Correlation between active muscle volume of the left (A) and right (B) sides with rate of body flexion as estimated from strain data measured in the left side. *y*-values are the same in A and B for a given feeding behavior because the rate of body flexion is presumably the same in the left and right sides during dorsiflexion used in feeding. We also include miscellaneous 'feeding' behaviors such as misdirected strikes at non-living objects and coughs that used dorsiflexion. Strain data for feeding could not be included for Lm03 due to malfunction of the dorsomedial transducer pair. (C,D) Locomotor behaviors. Regressions for locomotion were generated separately based on the direction of bending. In leftward bending (C), we correlated active muscle volume on the left side with rate of body flexion, as calculated by normalizing all leftward rates to the highest leftward rate. In rightward bending (D), we correlated the active muscle volume of the right side with rate of flexion as estimated using transducers in the left side, and then normalizing all rightward rates to the highest rightward rate. C and D use different *x*- and *y*-values because each data point represents flexion in a particular direction (toward the left or right). Thus, stage 1 behavior in C indicates stage 1 occurs as a flexion toward the left. Shapes and colors indicate data from different individuals and behaviors, respectively. Regression lines with 95% confidence intervals and statistics (adjusted r^2, number of observations and *P*-values) are shown for each panel.

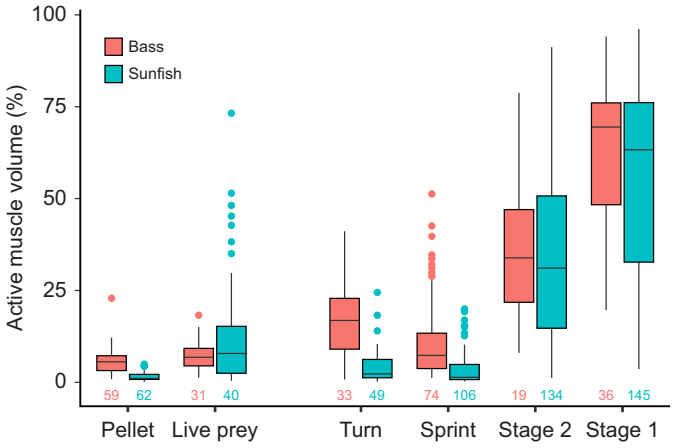

Fig. 7. Active muscle volume for different behaviors in sunfish and bass. Active muscle volume was estimated by taking the normalized activation intensity from three epaxial regions and weighing them by their relative cross-sectional area. Data from all individuals are pooled by species (*N*=4 for sunfish and *N*=3 for bass). The number of trials for each species and behavior category is listed at the bottom. Bass data from Jimenez and Brainerd (2020) were analyzed for this study.

likely to use the dorsal muscle regions for sprinting, (2) sunfish used activation intensities for prey strikes that were substantially higher than those for pellet strikes, whereas these were more similar in largemouth bass, (3) sunfish used activation intensities for the highest performance prey strikes that were similar to the highest activation intensities in fast-starts. Overall, the recruitment patterns observed in largemouth bass and bluegill sunfish are consistent with the epaxial neuroanatomy in fishes, described in zebrafish (*Danio rerio*) and goldfish (*Cyprinus carpio*), which consists of some motoneurons that innervate varying numbers of muscle fibers within a given epaxial region and other motoneurons that innervate spatially distinct epaxial regions (Bello-Rojas et al., 2019; Fetcho, 1987; Westerfield et al., 1986). Our observations and those made in prior anatomical and experimental studies suggest that teleost fishes possess the prerequisite neuroanatomy necessary for modulating swimming and suction-feeding performance through regionalized and graded recruitment of axial muscle.

Differences between bluegill sunfish and largemouth bass also suggest that active muscle volume is an important determinant of muscle mass-specific power output in suction feeding. Active muscle volume for sunfish and bass overlaps considerably (Fig. 7), coinciding with the overlapping muscle mass-specific power output generated by

the epaxial muscle of these species (Camp et al., 2018). Yet, at the highest levels of suction-feeding performance, sunfish and bass produce considerably different muscle power outputs and, as we found here, the highest recorded active muscle volumes are considerably greater in sunfish as compared with the highest values for bass (Fig. 7). For example, the highest recorded muscle mass-specific power for the axial muscle for sunfish in suction feeding (438 W kg^{-1}) is over 3 times greater than that recorded for bass (141 W kg^{-1}; Camp et al., 2018), and here we showed sunfish routinely used active muscle volumes 2–3 times greater than the highest value recorded in bass (see highest performance sunfish strikes on live prey in Fig. 7). Additionally, in sunfish, the relationship between active muscle volume and peak rate of body flexion – a continuous measure of performance – provides strong evidence that these high values of active muscle volume represent highly motivated behaviors (Fig. 6) rather than outliers due to methodological or analytic error. Demonstrating this relationship is important because highly motivated behaviors are known to be difficult to elicit in experimental settings (Astley et al., 2013; Moran et al., 2019). These findings suggest that although epaxial muscle is critical to suction feeding in both of these species, only some species may maximize the mechanical output of the muscle by activating all of it for suction feeding. Sunfish generate very high suction powers using epaxial activation intensities on par with fast-starts, whereas bass do not.

Active muscle volume and performance

The relationship between active muscle volume and peak rate of body flexion suggests that muscle recruitment drives performance for feeding and locomotion. This relationship is remarkable considering that these two functions involve different loading regimes (Day et al., 2005; Tytell and Lauder, 2008) and body movements (Jimenez et al., 2021), along with differences between locomotor behaviors such as sprinting and fast-starts (Tytell and Lauder, 2004). These data suggest that feeding performance in sunfish is modulated by activating a different number of muscle regions and a different number of muscle fibers with in each region, whereas locomotor performance is modulated primarily by activating a different number of muscle fibers as all three epaxial regions are almost always active (Fig. 3). Furthermore, it suggests that performance is partly responsible for variation within behavior categories (e.g. Fig. 5). Although our results suggest that active muscle volume is a reasonable estimate of muscular exertion, the exact relationships between active muscle volume, muscle output and organismal performance are unclear. This is likely due to the difficulty of using the EMG signal to infer muscle mechanics from the EMG signal (Roberts and Gabaldón, 2008) and the complexity of muscles contracting against dynamic loads such as those present in suction feeding and locomotion (Marsh, 1999; Richards, 2011). Nevertheless, in fishes, the strength of the EMG signal has been previously correlated to suction forces (Carroll and Wainwright, 2006; Jimenez and Brainerd, 2020) and tail-beat frequency (Jimenez and Brainerd, 2020). EMG signal strength has also been correlated with force and shortening velocity in bird flight (Hedrick et al., 2003), and with running speed in humans (Biewener et al., 2004). In this study and its counterpart (Jimenez and Brainerd, 2020), the well-established full activation of axial muscle during the escape behavior provides an intuitive way of normalizing the signal, as the percentage value approximates the relative number of muscle fibers active in a given region for a given behavior. Additionally, combining EMG data from multiple electrodes positioned in different muscle regions, while accounting for the size of each region, provides a more representative estimate of mechanical exertion in large muscles. Our analysis suggests that this metric is a powerful tool for comparative research, though future work should be done to explore in more detail the relationship between active muscle volume and organismal performance.

Mechanical implications of bilateral activation

Feeding and locomotion use distinct motor control strategies (Figs 3 and 4) and, consequently, different mechanical strategies (for bilateral asymmetry of muscle activity along the body, see Westneat et al., 1998, and Tytell and Lauder, 2002). Feeding and locomotion involve different muscle synergies, as each function requires axial muscle flexion within a different anatomical plane (Jimenez et al., 2018, 2021). In swimming, the left and right sides of the body are antagonistic: active shortening on one side (ipsilateral: positive work) tends to produce lengthening on the other side (contralateral: negative work). In suction feeding, the left and right sides of the body are synergistic, as both sides of the epaxial musculature must actively shorten (positive work) to elevate the neurocranium (for bilateral epaxial activity during ram feeding, see Lauder and Norton, 1980). Thus, if positive work production is unilateral for swimming but bilateral for feeding, it is plausible that high-performance suction feeding can produce higher net muscle power outputs than fast-starts. Although axial muscles on opposite sides of the body are necessarily antagonistic in locomotion, this arrangement may still provide performance advantages.

It has been speculated that the preparatory phase of the fast-start (stage 1) can enhance muscle mechanics of the propulsive phase (stage 2) (Franklin and Johnston, 1997; James and Johnston, 1998). Higher muscle power output, mechanical output, velocity and acceleration in stage-2 fast-starts provide evidence of enhancement (Altringham and Johnston, 1990; Frith and Blake, 1995; James and Johnston, 1998; Tytell and Lauder, 2008), although the specific mechanisms are unclear. One proposed mechanism is that of force enhancement via eccentric muscle contraction. As force production is enhanced when an active muscle is lengthened by its antagonist, the same contralateral muscle that actively lengthens during stage 1 produces higher muscle force and power when it actively shortens in stage 2 (Franklin and Johnston, 1997; James and Johnston, 1998). However, only a relatively small percentage of muscle fibers actively lengthen in swimming (Fig. 2), and any mechanical enhancement due to active lengthening would be limited to that smaller group of fibers. Thus, a hypothesis of enhanced muscle performance in stage 2 needs to account for active lengthening in a few fibers and passive lengthening in most fibers. An alternative hypothesis suggests that intramuscular pressure in the contralateral muscle enhances fast-start performance through elastic energy storage (Westneat et al., 1998), and not necessarily enhanced muscle performance. However, it should be noted that intramuscular pressure can also enhance contractile forces (Sleboda and Roberts, 2020).

Finally, contralateral muscle activity may be used to modulate body stiffness, force transmission and/or escape trajectory (Tytell et al., 2018; Westneat et al., 1998) – alternatives not necessarily related to enhancing muscle mechanics. Future studies are needed to more precisely test these hypotheses and to determine if the role of contralateral muscle activity varies across species with different body shapes and swimming modes (Altringham and Ellerby, 1999).

Patterns of muscle activation in fast-starts

Bluegill sunfish activated epaxial muscle bilaterally for fast-starts, but with higher activation intensities on the side of muscle shortening (Figs 2 and 6). Other fish species have also been shown to activate the axial muscle bilaterally for fast-starts, although muscle recruitment patterns for fast-starts can vary intraspecifically and interspecifically (Czuwala et al., 1999; Ellerby and Altringham, 2001; Hale, 2002;

Tytell and Lauder, 2002; Westneat et al., 1998). One example of this intraspecific variation is the muskellunge (*Esox masquinongy*), which activate muscle unilaterally along the whole body during stage 1 of C-starts, but activate muscle bilaterally in posterior regions during stage 1 of S-starts (Hale et al., 2002). Interspecific variation of bilateral muscle activity during C-starts ranges from some species using bilateral activity for some stages, to unilateral activity for other stages and, in some cases, no activity whatsoever in stage-2 fast-starts (Hale et al., 2002). In comparison, we show both qualitatively (Fig. 2B) and quantitatively (Fig. 3B) that bluegill sunfish activate ipsilateral and contralateral muscle during both stages of the fast-start. These intraspecific and interspecific differences may be a result of the diverse neural circuits used for initiating fast-starts (Liu and Hale, 2014), but we suspect that methodological factors are also important. Here, we used a thresholding method to determine whether muscle was active, whereas other studies used different methods. In some cases, EMG bursts with very low peak voltages that would have been reasonably ruled out as inactive in other studies may have been included as active in our analysis. Although these methodological and biological factors may yield different results and interpretations, it is worth noting that these studies consistently found higher levels of muscle activity on the side of muscle shortening as compared to the side of muscle lengthening for fast-starts (Fig. 3).

Functional diversity of muscle activation

Species from various vertebrate taxa have been shown to modulate muscle activity in response to variable conditions and for different behaviors (Azizi et al., 2008; Biewener and Gillis, 1999; Carr et al., 2011; Gillis and Biewener, 2000; Roberts et al., 2007). In fishes, motor control of the axial musculature has been studied primarily in relation to locomotor function, corresponding to a tradition of interpreting musculoskeletal anatomy, physiology and mechanics primarily through the lens of axial locomotion. Considering that locomotion is the ancestral function of the axial musculoskeletal system (Fletcher et al., 2014; Webb, 1982), such an approach has yielded critical insights into the form–function relationships of fish locomotion. Yet, the emerging multifunctional perspective for fish axial musculature cautions against automatically assuming musculoskeletal traits are locomotor adaptations. The evidence suggests that most suction-feeding fish can activate all epaxial regions (Camp et al., 2015, 2018; Jimenez and Brainerd, 2020), and that even a fish species with a relatively common mouth and body shape, bluegill sunfish, may be capable of activating the entire muscle volume at 35% SL in high-performance suction feeding. How does this affect our understanding of and approach to the axial musculature of fishes?

In largemouth bass, high muscle recruitment in high-performance swimming and low muscle recruitment in suction feeding provide evidence that the axial musculature is primarily suited for swimming. If all fish used the axial muscle like bass, then it would strongly support the historical perspective that this is primarily a swimming muscle. The similar levels of muscle recruitment in high-performance swimming and high-performance suction feeding in bluegill sunfish provide a counter example to the historical locomotor perspective. Our discovery that high-performance swimming and suction feeding can use similar levels of muscle recruitment suggests that either biological function could be the subject of natural selection on epaxial muscle structure and mechanical function. Elucidating the functional specialization of this muscle may require exploration into its architecture and physiology, as well as *in vitro* experiments that simulate muscle performance under the strain–activation conditions observed in both functions.

Acknowledgements

We are grateful to Thomas Roberts, Richard Marsh and Andrew Biewener for their guidance on this project and valuable comments on the manuscript. We also thank Dave Ellerby for his help with collecting animals; Jake Parsons, Jarrod Petersen and Amy Rutter for assistance with surgeries; Erika Tavares for research administrative support.

Competing interests

The authors declare no competing or financial interests.

Author contributions

Conceptualization: Y.E.J., E.L.B.; Methodology: Y.E.J.; Validation: Y.E.J.; Formal analysis: Y.E.J.; Investigation: Y.E.J.; Data curation: Y.E.J.; Writing - original draft: Y.E.J.; Writing - review & editing: Y.E.J., E.L.B.; Visualization: Y.E.J.; Project administration: E.L.B.; Funding acquisition: Y.E.J., E.L.B.

Funding

This research was supported by National Science Foundation (NSF) grants 1655756 and 1661129 to E.L.B., a Doctoral Dissertation Enhancement Grant from the Bushnell Graduate Education and Research Fund to Y.E.J. and a National Science Foundation Graduate Research Fellowship to Y.E.J.

Data availability

Video, EMG and sonomicrometry data are available from ZMAPortal (zmaportal.org), study 'Sunfish EMG and Sonomicrometry in Feeding and Locomotion', permanent ID ZMA27.

References

Alexander, R. M. N. (1969). The orientation of muscle fibres in the myomeres of fishes. *J. Mar. Biol. Assoc. U. K.* **49**, 263-290. doi:10.1017/S0025315400035906

Altringham, J. D. and Ellerby, D. J. (1999). Fish swimming: patterns in muscle function. *J. Exp. Biol.* **202**, 3397-3403. doi:10.1242/jeb.202.23.3397

Altringham, J. D. and Johnston, I. A. (1990). Modelling muscle power output in a swimming fish. *J. Exp. Biol.* **148**, 395-402. doi:10.1242/jeb.148.1.395

Astley, H. C., Abbott, E. M., Azizi, E., Marsh, R. L. and Roberts, T. J. (2013). Chasing maximal performance: a cautionary tale from the celebrated jumping frogs of Calaveras County. *J. Exp. Biol.* **216**, 3947-3953. doi:10.1242/jeb.090357

Azizi, E., Brainerd, E. L. and Roberts, T. J. (2008). Variable gearing in pennate muscles. *Proc. Natl. Acad. Sci. USA* **105**, 1745-1750. doi:10.1073/pnas.0709212105

Bainbridge, R. (1958). The speed of swimming of fish as related to size and to the frequency and amplitude of the tail beat. *J. Exp. Biol.* **35**, 109-133. doi:10.1242/jeb.35.1.109

Bello-Rojas, S., Istrate, A. E., Kishore, S. and McLean, D. L. (2019). Central and peripheral innervation patterns of defined axial motor units in larval zebrafish. *J. Comp. Neurol.* **527**, 2557-2572. doi:10.1002/cne.24689

Biewener, A. A. and Corning, W. R. (2001). Dynamics of mallard (*Anas platyrynchos*) gastrocnemius function during swimming versus terrestrial locomotion. *J. Exp. Biol.* **204**, 1745-1756. doi:10.1242/jeb.204.10.1745

Biewener, A. A. and Gillis, G. B. (1999). Dynamics of muscle function during locomotion: accommodating variable conditions. *J. Exp. Biol.* **202**, 3387-3396. doi:10.1242/jeb.202.23.3387

Biewener, A. A., Farley, C. T., Roberts, T. J. and Temaner, M. (2004). Muscle mechanical advantage of human walking and running: implications for energy cost. *J. Appl. Physiol.* **97**, 2266-2274. doi:10.1152/japplphysiol.00003.2004

Boddeke, R., Slijper, E. J. and Van Der Stelt, A. (1959). Histological characteristics of the body musculature of fishes in connection with their mode of life. *Proc. K. Ned. Akad. van Wet.* **62**, 576-588.

Bone, Q., Joe, K. W. and Jones, D. R. (1978). On the role of the different fibre types in fish myotomes at intermediate swimming speeds. *Fish. Bull.* **76**, 691-699.

Brainerd, E. L., Blob, R. W., Hedrick, T. L., Creamer, A. T. and Müller, U. K. (2017). Data management rubric for video data in organismal biology. *Integr. Comp. Biol.* **57**, 33-47. doi:10.1093/icb/icx060

Camp, A. L. and Brainerd, E. L. (2014). Role of axial muscles in powering mouth expansion during suction feeding in largemouth bass (*Micropterus salmoides*). *J. Exp. Biol.* **217**, 1333-1345. doi:10.1242/jeb.095810

Camp, A. L., Roberts, T. J. and Brainerd, E. L. (2015). Swimming muscles power suction feeding in largemouth bass. *Proc. Natl. Acad. Sci. USA* **112**, 8690-8695. doi:10.1073/pnas.1508055112

Camp, A. L., Roberts, T. J. and Brainerd, E. L. (2018). Bluegill sunfish use high power outputs from axial muscles to generate powerful suction-feeding strikes. *J. Exp. Biol.* **221**, jeb178160. doi:10.1242/jeb.178160

Camp, A. L., Olsen, A. M., Hernandez, L. P. and Brainerd, E. L. (2020). Fishes can use axial muscles as anchors or motors for powerful suction feeding. *J. Exp. Biol.* **223**, jeb225649. doi:10.1242/jeb.225649

Carr, J. A., Ellerby, D. J. and Marsh, R. L. (2011). Function of a large biarticular hip and knee extensor during walking and running in Guinea fowl (*Numida meleagris*). *J. Exp. Biol.* **214**, 3405-3413. doi:10.1242/jeb.060335

Carroll, A. M. and Wainwright, P. C. (2006). Muscle function and power output during suction feeding in largemouth bass, *Micropterus salmoides*. *Comp. Biochem. Physiol. A. Mol. Integr. Physiol.* **143**, 389-399. doi:10.1016/j.cbpa.2005.12.022
Carroll, A. M., Wainwright, P. C., Huskey, S. H., Collar, D. C. and Turingan, R. G. (2004). Morphology predicts suction feeding performance in centrarchid fishes. *J. Exp. Biol.* **207**, 3873-3881. doi:10.1242/jeb.01227
Carroll, A. M., Ambrose, A. M., Anderson, T. A. and Coughlin, D. J. (2009). Feeding muscles scale differently from swimming muscles in sunfish (Centrarchidae). *Biol. Lett.* **5**, 274-277. doi:10.1098/rsbl.2008.0647
Coughlin, D. J. and Rome, L. C. (1996). The roles of pink and red muscle in powering steady swimming in scup, *Stenotomus chrysops*. *Am. Zool.* **36**, 666-677. doi:10.1093/icb/36.6.666
Czuwala, P. J., Blanchette, C., Varga, S., Root, R. G. and Long, J. H. (1999). A mechanical model for the rapid body flexures of fast-starting fish. Proc. 11th Int. Symp. Unmanned Untethered Submersible Technology 415-426.
Day, S. W., Higham, T. E., Cheer, A. Y. and Wainwright, P. C. (2005). Spatial and temporal patterns of water flow generated by suction-feeding bluegill sunfish *Lepomis macrochirus* resolved by particle image velocimetry. *J. Exp. Biol.* **208**, 2661-2671. doi:10.1242/jeb.01708
Ellerby, D. J. and Altringham, J. D. (2001). Spatial variation in fast muscle function of the rainbow trout *Oncorhynchus mykiss* during fast-starts and sprinting. *J. Exp. Biol.* **204**, 2239-2250. doi:10.1242/jeb.204.13.2239
Ellerby, D. J., Spierts, I. L. Y. and Altringham, J. D. (2001). Fast muscle function in the European eel (*Anguilla anguilla* L.) during aquatic and terrestrial locomotion. *J. Exp. Biol.* **204**, 2231-2238. doi:10.1242/jeb.204.13.2231
Fetcho, J. R. (1987). A review of the organization and evolution of motoneurons innervating the axial musculature of vertebrates. *Brain Res. Rev.* **12**, 243-280. doi:10.1016/0165-0173(87)90001-4
Fletcher, T., Altringham, J., Peakall, J., Wignall, P. and Dorrell, R. (2014). Hydrodynamics of fossil fishes. *Proc. R. Soc. B Biol. Sci.* **281**, 20140703. doi:10.1098/rspb.2014.0703
Franklin, C. E. and Johnston, I. A. (1997). Muscle power output during escape responses in an antarctic fish. *J. Exp. Biol.* **200**, 703-712. doi:10.1242/jeb.200.4.703
Frith, H. and Blake, R. (1995). The mechanical power output and hydromechanical efficiency of northern pike (*Esox lucius*) fast-starts. *J. Exp. Biol.* **198**, 1863-1873. doi:10.1242/jeb.198.9.1863
Fuxjager, M. J., Fusani, L., Goller, F., Trost, L., Maat, A. T., Gahr, M., Chiver, I., Ligon, R. M., , IV, Chew, J. and Schlinger, B. A. (2017). Neuromuscular mechanisms of an elaborate wing display in the golden-collared manakin (*Manacus vitellinus*). *J. Exp. Biol.* **220**, 4681-4688. doi:10.1242/jeb.167270
Gemballa, S. and Vogel, F. (2002). Spatial arrangement of white muscle fibers and myoseptal tendons in fishes. *Comp. Biochem. Physiol. A Mol. Integr. Physiol.* **133**, 1013-1037. doi:10.1016/S1095-6433(02)00186-1
Gillis, G. B. and Biewener, A. A. (2000). Hindlimb extensor muscle function during jumping and swimming in the toad (*Bufo marinus*). *J. Exp. Biol.* **203**, 3547-3563. doi:10.1242/jeb.203.23.3547
Greer-Walker, M. and Pull, G. A. (1975). A survey of red and white muscle in marine fish. *J. Fish Biol.* **7**, 295-300. doi:10.1111/j.1095-8649.1975.tb04602.x
Hale, M. E. (2002). S- and C-start escape responses of the muskellunge (*Esox masquinongy*) require alternative neuromotor mechanisms. *J. Exp. Biol.* **205**, 2005-2016. doi:10.1242/jeb.205.14.2005
Hale, M. E., Long, J. H., , Jr., McHenry, M. J. and Westneat, M. W. (2002). Evolution of behavior and neural control of the fast-start escape response. *Evolution* **56**, 993-1007. doi:10.1111/j.0014-3820.2002.tb01411.x
Hedrick, T. L., Tobalske, B. W. and Biewener, A. A. (2003). How cockatiels (*Nymphicus hollandicus*) modulate pectoralis power output across flight speeds. *J. Exp. Biol.* **206**, 1363-1378. doi:10.1242/jeb.00272
Henneman, E. (1957). Relation between size of neurons and their susceptibility to discharge. *Science* **126**, 1345-1347. doi:10.1126/science.126.3287.1345
Henneman, E., Somjen, G. and Carpenter, D. O. (1965). Functional significance of cell size in spinal motoneurons. *J. Neurophysiol.* **28**, 560-580. doi:10.1152/jn.1965.28.3.560
Higham, T. E. (2007). Feeding, fins and braking maneuvers: locomotion during prey capture in centrarchid fishes. *J. Exp. Biol.* **210**, 107-117. doi:10.1242/jeb.02634
James, R. and Johnston, I. A. (1998). Scaling of muscle performance during escape responses in the fish *Myoxocephalus scorpius* L. *J. Exp. Biol.* **201**, 913-923. doi:10.1242/jeb.201.7.913
Jayne, B. C. and Lauder, G. V. (1994). How swimming fish use slow and fast muscle fibers: implications for models of vertebrate muscle recruitment. *J. Comp. Physiol. A* **175**, 123-131. doi:10.1007/BF00217443
Jayne, B. C., Bennett, A. F. and Lauder, G. V. (1990). Muscle recruitment during terrestrial locomotion: how speed and temperature affect fibre type use in a lizard. *J. Exp. Biol.* **152**, 101-128. doi:10.1242/jeb.152.1.101
Jimenez, Y. E., Camp, A. L., Grindall, J. D. and Brainerd, E. L. (2018). Axial morphology and 3D neurocranial kinematics in suction-feeding fishes. *Biology Open* **7**, bio036335. doi:10.1242/bio.036335
Jimenez, Y. E. and Brainerd, E. L. (2020). Dual function of epaxial musculature for swimming and suction feeding in largemouth bass. *Proc. R. Soc. B Biol. Sci.* **287**, 20192631. doi:10.1098/rspb.2019.2631
Jimenez, Y. E., Marsh, R. L. and Brainerd, E. L. (2021). A biomechanical paradox in fish: swimming and suction feeding produce orthogonal strain gradients in the axial musculature. *Sci. Rep.* **11**, 10334. doi:10.1038/s41598-021-88828-x
Johnston, I. A., Davison, W. and Goldspink, G. (1977). Energy metabolism of carp swimming muscles. *J. Comp. Physiol.* **114**, 203-216. doi:10.1007/BF00688970
Lauder, G. V. (1980). Evolution of the feeding mechanism in primitive actionopterygian fishes: a functional anatomical analysis of *Polypterus*, *Lepisosteus*, and *Amia*. *J. Morphol.* **163**, 283-317. doi:10.1002/jmor.1051630305
Lauder, G. V., , Jr. and Norton, S. M. (1980). Asymmetrical muscle activity during feeding in the gar, *Lepisosteus oculatus*. *J. Exp. Biol.* **84**, 17-32. doi:10.1242/jeb.84.1.17
Liu, Y.-C. and Hale, M. E. (2014). Alternative forms of axial startle behaviors in fishes. *Zoology* **117**, 36-47. doi:10.1016/j.zool.2013.10.008
Longo, S. J., McGee, M. D., Oufiero, C. E., Waltzek, T. B. and Wainwright, P. C. (2016). Body ram, not suction, is the primary axis of suction-feeding diversity in spiny-rayed fishes. *J. Exp. Biol.* **219**, 119-128. doi:10.1242/jeb.129015
Marsh, R. L. (1999). How muscles deal with real-world loads: the influence of length trajectory on muscle performance. *J. Exp. Biol.* **202**, 3377-3385. doi:10.1242/jeb.202.23.3377
Marsh, R. L. (2016). Speed of sound in muscle for use in sonomicrometry. *J. Biomech.* **49**, 4138-4141. doi:10.1016/j.jbiomech.2016.10.024
McLean, D. L., Fan, J., Higashijima, S.-I., Hale, M. E. and Fetcho, J. R. (2007). A topographic map of recruitment in spinal cord. *Nature* **446**, 71-75. doi:10.1038/nature05588
Moran, C. J., Rzucidlo, C. L., Ellerby, D. J. and Gerry, S. P. (2019). Laboratory constraints on feeding behaviours in polymorphic bluegill sunfish (*Lepomis macrochirus*). *Freshw. Biol.* **64**, 926-932. doi:10.1111/fwb.13274
Nemeth, D. (1997). Modulation of buccal pressure during prey capture in *Hexagrammos decagrammus* (Teleostei: Hexagrammidae). *J. Exp. Biol.* **200**, 2145-2154. doi:10.1242/jeb.200.15.2145
Norton, S. F. and Brainerd, E. L. (1993). Convergence in the feeding mechanics of ecomorphologically similar species in the Centrarchidae and Cichlidae. *J. Exp. Biol.* **176**, 11-29. doi:10.1242/jeb.176.1.11
Olson, J. M. and Marsh, R. L. (1998). Activation patterns and length changes in hindlimb muscles of the bullfrog *Rana catesbeiana* during jumping. *J. Exp. Biol.* **201**, 2763-2777. doi:10.1242/jeb.201.19.2763
Oufiero, C. E., Holzman, R. A., Young, F. and Wainwright, P. C. (2012). New insights from serranid fishes on the role of trade-offs in suction-feeding diversification. *J. Exp. Biol.* **215**, 3845-3855. doi:10.1242/jeb.074849
Richards, C. T. (2011). Building a robotic link between muscle dynamics and hydrodynamics. *J. Exp. Biol.* **214**, 2381-2389. doi:10.1242/jeb.056671
Roberts, T. J. and Gabaldón, A. M. (2008). Interpreting muscle function from EMG: lessons learned from direct measurements of muscle force. *Integr. Comp. Biol.* **48**, 312-320. doi:10.1093/icb/icn056
Roberts, T. J., Higginson, B. K., Nelson, F. E. and Gabaldón, A. M. (2007). Muscle strain is modulated more with running slope than speed in wild turkey knee and hip extensors. *J. Exp. Biol.* **210**, 2510-2517. doi:10.1242/jeb.003913
Sleboda, D. A. and Roberts, T. J. (2020). Internal fluid pressure influences muscle contractile force. *Proc. Natl. Acad. Sci. USA* **117**, 1772-1778. doi:10.1073/pnas.1914433117
Thys, T. (1997). Spatial variation in epaxial muscle activity during prey strike in largemouth bass (*Micropterus salmoides*). *J. Exp. Biol.* **200**, 3021-3031. doi:10.1242/jeb.200.23.3021
Tytell, E. D. and Lauder, G. V. (2002). The C-start escape response of *Polypterus senegalus*: bilateral muscle activity and variation during stage 1 and 2. *J. Exp. Biol.* **205**, 2591-2603. doi:10.1242/jeb.205.17.2591
Tytell, E. D. and Lauder, G. V. (2004). The hydrodynamics of eel swimming: I. Wake structure. *J. Exp. Biol.* **207**, 1825-1841. doi:10.1242/jeb.00968
Tytell, E. D. and Lauder, G. V. (2008). Hydrodynamics of the escape response in bluegill sunfish, *Lepomis macrochirus*. *J. Exp. Biol.* **211**, 3359-3369. doi:10.1242/jeb.020917
Tytell, E. D., Carr, J. A., Danos, N., Wagenbach, C., Sullivan, C. M., Kiemel, T., Cowan, N. J. and Ankarali, M. M. (2018). Body stiffness and damping depend sensitively on the timing of muscle activation in lampreys. *Integr. Comp. Biol.* **58**, 860-873. doi:10.1093/icb/icy042
Van Wassenbergh, S., Herrel, A., Adriaens, D. and Aerts, P. (2005). A test of mouth-opening and hyoid-depression mechanisms during prey capture in a catfish using high-speed cineradiography. *J. Exp. Biol.* **208**, 4627-4639. doi:10.1242/jeb.01919
Wardle, C. S. (1975). Limit of fish swimming speed. *Nature* **255**, 725-727. doi:10.1038/255725a0
Webb, P. W. (1982). Locomotor patterns in the evolution of actinopterygian fishes. *Am. Zool.* **22**, 329-342. doi:10.1093/icb/22.2.329
Westerfield, M., McMurray, J. V. and Eisen, J. S. (1986). Identified motoneurons and their innervation of axial muscles in the zebrafish. *J. Neurosci.* **6**, 2267-2277. doi:10.1523/JNEUROSCI.06-08-02267.1986
Westneat, M. W., Hale, M. E., McHenry, M. J. and Long, J. H., Jr. (1998). Mechanics of the fast-start: Muscle function and the role of intramuscular pressure in the escape behavior of *Amia calva* and *Polypterus palmas*. *J. Exp. Biol.* **201**, 3041-3055. doi:10.1242/jeb.201.22.3041